

Enhanced atomic corrugation in dynamic force microscopy—The role of repulsive forces

L. Lichtenstein, C. Büchner, S. Stuckenholtz, M. Heyde,^{a)} and H.-J. Freund
Fritz-Haber-Institut der Max-Planck-Gesellschaft, Faradayweg 4-6, D-14195 Berlin, Germany

(Received 15 November 2011; accepted 2 March 2012; published online 22 March 2012)

Full range two dimensional (2D) force mapping was performed by means of low temperature dynamic force microscopy (DFM) on a highly complex surface structure. For this purpose, we used a thin film of vitreous silica on a Ru(0001)-support, which is a 2D structural equivalent to silica glass. The 2D spectroscopy shows that the contrast generating shift in vertical distance between two sites on the surface is twice as large on the repulsive branch of the frequency shift-distance curve as compared to the attractive branch. The results give insight into the origin of the formation of atomic resolution in DFM. © 2012 American Institute of Physics.

[<http://dx.doi.org/10.1063/1.3696039>]

Atomic force microscopy (AFM) has shown the capability of resolving the atomic structure of various surfaces. Especially when using dynamic force microscopy (DFM)—also called noncontact AFM (nc-AFM)—it is possible to observe true atomic resolution of molecules,¹ thin films,² metals,³ semiconductors,⁴ and insulators.^{5,6} However, some surfaces are hard to image with constant frequency shift (Δf) DFM. This issue is connected with the exact shape of the energetical landscape. By means of two dimensional (2D) or three dimensional (3D) force mapping, it is possible to measure these landscapes and it therefore provides detailed insight into the contrast mechanisms of DFM.

In this paper, we report on 2D force mapping on a complex surface structure. A prominent example of a complex atomic structure is silica glass. Silica glass is an extensively studied material (see Ref. 7 and references therein). Yet, detailed knowledge about the atomic arrangement in amorphous solids remains scarce. For this reason, we chose a thin vitreous silica film on a Ru support for our investigations. Recently, we reported on the atomic structure of a thin vitreous silica film on Ru(0001).⁸ Shortly after, the existence of a thin silica glass was shown on graphene.⁹ These films reproduce the main structural properties of vitreous bulk silica and are therefore promising model systems, e.g., for catalysis. Furthermore, using DFM one can probe substrate-adsorbate interactions, because the tip termination can be seen as a model of an adatom probing specific adsorption sites.

To acquire 2D or 3D spectroscopy with DFM, one needs to measure Δf as a function of the three space coordinates (x , y , and z) above the selected scan area of the surface.^{10–12} In principle, the tip can be moved in either space direction first. Technically, difficulties may arise when leveling separate $\Delta f(z)$ -curves or if significant drift is involved. In this study, we chose to perform 2D Δf -spectroscopy with the fast scan direction parallel to the surface, because we want to focus on the imaging process at varying heights and Δf -values. In addition to the space coordinates, it is also possible to vary the bias voltage to gain information about electrostatic effects.¹³ The force between tip and sample can be calcu-

lated from Δf using the equations in Ref. 14. As we are interested in the signal for the z -feedback loop used for topographic imaging, we restrict ourselves to the discussion of Δf .

In this study, we applied a custom-built dual mode microscope which combines DFM and scanning tunneling microscopy (STM) using a tuning fork sensor. The microscope is operated at low temperatures (5 K) in ultra high vacuum (UHV). Details about the setup can be found in our previous publications.^{15,16} Thanks to high stability and low drift, the setup is capable of performing high resolution 2D Δf -mapping.¹⁷

The vitreous silica film was prepared by evaporating Si from a Si rod onto a 3O-(2 × 2)-precovered Ru(0001)-surface in an O₂ atmosphere of 2×10^{-7} mbar. Subsequently, the sample was annealed at 950 °C in 5×10^{-6} mbar O₂ leading to an extended and atomically flat vitreous silica double layer sheet.

Fig. 1 presents two high resolution images of the vitreous silica film. Both images were acquired simultaneously in the constant height mode. Fig. 1(a) shows a map of tunneling current (I_T) and Fig. 1(b) a map of Δf . The I_T - and the Δf -map reveal a complex arrangement of protrusions. From the true atomic resolution in Fig. 1(b), an atomic model of the film can be constructed. We assign the protrusions in Fig. 1(b) to the O positions of the silica film's topmost layer because only O exhibits a triangular symmetry. The Si positions are obtained by calculating the center of every O triangle. The resulting model of the topmost Si and O-layer is superimposed onto the constant height pictures in the lower left corner. We observed atoms arranged in SiO₄-tetrahedra (short range order), which form a ring network (medium range order). The size of the rings ranged from four to nine Si atoms per ring. For a detailed statistical analysis of the film structure, see Ref. 8.

This atomically resolved data served as a starting point for the 2D Δf -spectroscopy. We subsequently recorded Δf along a lateral 3 nm-long line (white dotted lines in Fig. 1) at increasing tip-sample separations. A vertical distance of 0 nm was defined for the height at which the constant height images were recorded. To ensure high data point density

^{a)}Electronic mail: heyde@fhi-berlin.mpg.de.

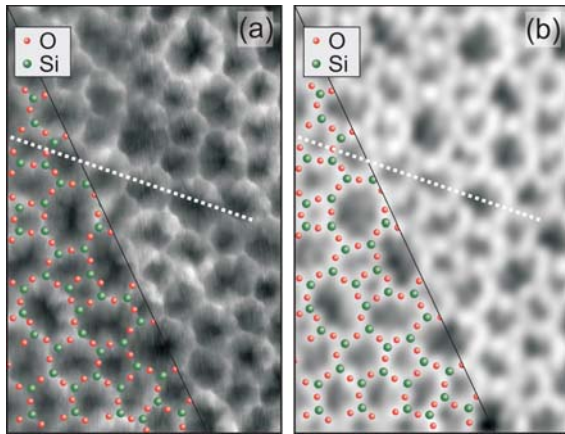


FIG. 1. (Color online) High resolution imaging of a thin vitreous silica film at constant height. (a) I_T -map. I_T -values ranged from 59 pA to 425 pA. (b) Δf -map. Δf -values ranged from -3.29 Hz to 0.25 Hz. The tuning fork oscillation amplitude was set to 0.27 nm. (a) and (b) Scan area = 3.2 nm \times 5 nm, $V_S = 100$ mV. White dotted lines indicate the position of the 2D spectroscopy.

close to the surface (around the minimum of the Δf -curve), we started with a small height difference of 5 pm and then gradually increased it to 0.5 nm. Finally, we obtained a 2D map of Δf vs. the lateral distance (x) and the vertical distance (z). Directly after the acquisition of $\Delta f(x, z)$, we scanned the surface again and we observed exactly the same atomic resolution imaging contrast. This proves that the microscopic tip termination remained the same during spectroscopy.

Fig. 2(a) shows two $\Delta f(z)$ -curves which were extracted from the Δf -map. The red data points correspond to $\Delta f(z)$ on top of a pore (Δ) and the blue curve to $\Delta f(z)$ on top of an O-atom (\circ). The inset shows a zoom-in on the short range regime marked by a gray box in Fig. 2(a). The two curves plotted exhibit a different behavior around the Δf -minimum (0.0 nm to 0.3 nm). On the attractive branch (positive slope of Δf ; abbreviated AB), the z -shift is small (10 to 30 pm). However, on the repulsive branch (negative slope of Δf ; abbreviated RB), the z -difference is large (80 to 120 pm). Consequently, the z -corrugation during constant Δf imaging is bigger on the RB than on the AB, e.g., for a Δf -setpoint of -1.6 Hz (dotted horizontal line).^{18,24} Constant height imaging is also more promising on the RB as the Δf -shift for a fixed z distance is bigger on the RB than on the AB.

The dissipation channel did not show any variation and no indications of tip-sample distortions were observed.^{19,20}

The simultaneously recorded $I_T(z)$ -curves are plotted in Fig. 2(b). The O-site curve clearly shows that when the tunneling regime ($I_T(z) > 10$ pA) is reached close to the surface, Δf is still on the AB. However, if we approach the tip closer to the surface and Δf passes at the minimum from the AB to the RB, $I_T(z)$ has a value of 50 pA. Thus, even at low I_T -values, Δf is already on the RB. It is also important to note that the atomic corrugation in Fig. 1(b) was recorded on the RB of Δf .

The difference between the AB and the RB is also visible in the 2D Δf -map depicted in Fig. 2(c). In this plot, the color scale reflects the value of Δf . We used linear interpolation to visualize the areas between the discontinuous horizontal $\Delta f(x)$ -lines. The vertical dotted lines indicate the positions of the extracted $\Delta f(z)$ - and $I_T(z)$ -curves in Figs. 2(a) and 2(b). The bottom of the plot gives information about the short range

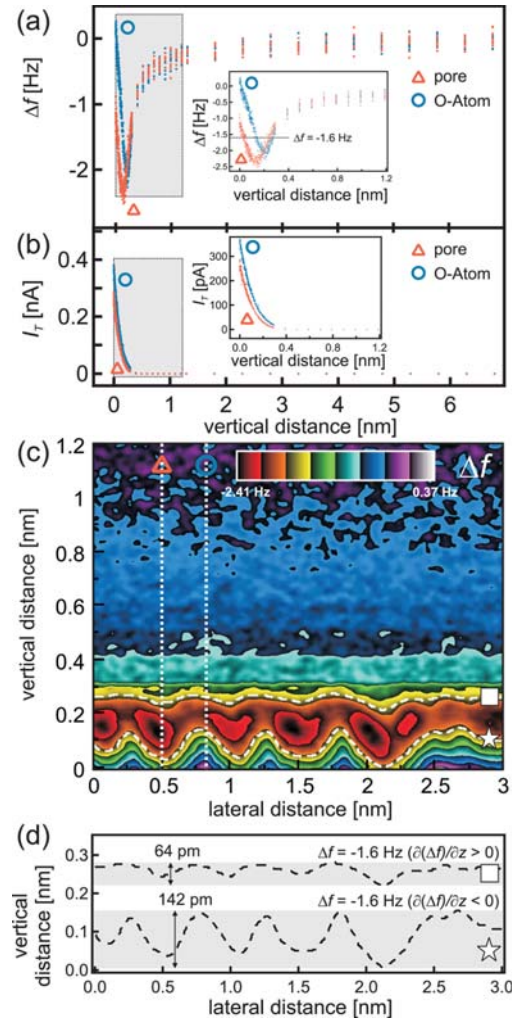


FIG. 2. (Color online) Evaluation of the 2D spectroscopy. (a) Two $\Delta f(z)$ -spectra taken from the 2D Δf -map. The inset shows a zoom-in on the gray shaded area. The $[\Delta]$ -marked curve was acquired above a pore (red color in the online version) and the $[\circ]$ -marked curve above an O-atom (blue color). (b) The $I_T(z)$ -spectra, which were simultaneously acquired with Δf . The inset shows a zoom-in on the gray shaded area. Same symbols as in (a). (c) $\Delta f(x, z)$ -image with the color scale showing the Δf -value. Dotted lines indicate the positions of the $\Delta f(z)$ - and $I_T(z)$ -spectra presented in (a) and (b). Dashed lines indicate contours of constant Δf ($\Delta f = -1.6$ Hz). $V_S = 100$ mV. Oscillation amplitude = 0.27 nm. (d) Two $z(x)$ -contours at constant Δf ($\Delta f = -1.6$ Hz; same as indicated in (c) by dashed lines). \square denotes the contour on the AB and $*$ the contour on the RB.

behavior of Δf along the horizontal scan line. The two dashed lines show contours of constant Δf ($\Delta f = -1.6$ Hz). Strikingly, the contour on the RB ($*$) shows a higher corrugation as compared to the AB (\square). To better quantify this difference, both contours are plotted in a separate graph (see Fig. 2(d)). The maximal corrugation on the AB is 64 pm, whereas the maximal corrugation on the RB is 142 pm. Thus, the corrugation on the RB is more than doubled compared with the one on the AB and leads to an enhanced imaging contrast.²¹ These findings are in line with the observation made by Mohn *et al.* on top of a pentacene molecule: on the AB the contour of constant Δf is quite flat, whereas on the RB the contour exhibits a corrugation revealing the positions of the five carbon rings.²²

To better understand the mechanisms of atomic resolution in constant Δf DFM, it is important to look at characteristic

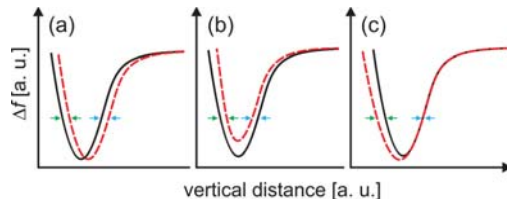


FIG. 3. (Color online) Different cases of $\Delta f(z)$ -curves for two surface sites (solid black and dashed red). (a) The dashed curve's minimum is shifted to larger tip-sample distances. (b) The minimum of the dashed curve is shifted to larger $\Delta f(z)$ -values. (c) The solid and the dashed curve show comparable characteristics on the AB. However, on the RB, they split up. (a)-(c) The arrow pairs show the absolute corrugation for a certain Δf -setpoint on the AB and RB (blue color represents the AB and green color the RB in the online version).

$\Delta f(z)$ -curves.²³ Different cases can exist, depending on the exact tip geometry as well as on the topographic, electronic, and chemical surface properties. Fig. 3 sketches three examples of $\Delta f(z)$ -curve shapes for two different surface sites (solid black and dashed red), e.g., top and hollow site of a fcc(100)-lattice. To observe a contrast in constant Δf DFM between these two sites, the curves must split up. This splitting can express itself in, e.g., a shift of the minimum to higher z (Fig. 3(a); like on NaCl in Ref. 22) or to higher Δf (Fig. 3(b); like on MgO in Ref. 17). These two cases allow imaging on the AB and on the RB with similar absolute corrugation. However, in case of Fig. 3(b), a contrast inversion occurs when switching the regimes, because the z -shift changes its sign. Another possibility is shown in Fig. 3(c). In this case, the characteristics of the red curve on the AB are very similar to the black curve. However, on the RB the two curves split up. This is in agreement with the $\Delta f(z)$ -curves presented in this paper. At constant Δf , one would only see an atomically resolved contrast on the RB, not on the AB.

In summary, we performed 2D spectroscopy on a metal supported thin vitreous silica film. Before and after the 2D Δf -mapping, we scanned the surface with the same atomic imaging contrast, proving that the tip configuration remained the same during spectroscopy. The $\Delta f(z)$ -curves extracted from the 2D data exhibited a clear z -deviation on the RB but not on the AB. The simultaneously acquired I_T - and Δf -signals demonstrated that even at moderate tunneling conditions the tip is so close to the surface that Δf is on the RB. Further, the

2D map clearly illustrated the difference between the AB and the RB of Δf . The z -corrugation was found to be more than twice as large on the RB compared to the AB. So, depending on the exact $\Delta f(z)$ -shape, atomic resolution in DFM might be hidden in the repulsive regime.

- ¹L. Gross, F. Mohn, N. Moll, P. Liljeroth, and G. Meyer, *Science* **325**, 1110 (2009).
- ²C. Loppacher, M. Bammerlin, M. Guggisberg, F. Battiston, R. Bennewitz, S. Rast, A. Baratoff, E. Meyer, and H.-J. Güntherodt, *Appl. Surf. Sci.* **140**, 287 (1999).
- ³S. Orisaka, T. Minobe, T. Uchihashi, Y. Sugawara, and S. Morita, *Appl. Surf. Sci.* **140**, 243 (1999).
- ⁴F. J. Giessibl, *Science* **267**, 68 (1995).
- ⁵C. Barth and M. Reichling, *Nature* **414**, 54 (2001).
- ⁶J. V. Lauritsen and M. Reichling, *J. Phys. Condens. Matter* **22**, 263001 (2010).
- ⁷G. N. Greaves and S. Sen, *Adv. Phys.* **56**, 1 (2007).
- ⁸L. Lichtenstein, C. Büchner, B. Yang, S. Shaikhutdinov, M. Heyde, M. Sierka, R. Włodarczyk, J. Sauer, and H.-J. Freund, *Angew. Chem. Int. Ed.* **51**, 404 (2012).
- ⁹P. Y. Huang, S. Kurasch, A. Srivastava, V. Skakalova, J. Kotakoski, A. V. Krashenninnikov, R. Hovden, Q. Mao, J. C. Meyer, J. Smet *et al.* *Nano Lett.* **12**, 1081 (2012).
- ¹⁰H. Hölscher, S. M. Langkat, A. Schwarz, and R. Wiesendanger, *Appl. Phys. Lett.* **81**, 4428 (2002).
- ¹¹B. J. Albers, T. C. Schwendemann, M. Z. Baykara, N. Pilet, M. Liebmann, E. I. Altman, and U. D. Schwarz, *Nanotechnology* **20**, 264002 (2009).
- ¹²M. Z. Baykara, T. C. Schwendemann, E. I. Altman, and U. D. Schwarz, *Adv. Mater.* **22**, 2838 (2010).
- ¹³T. König, L. Heinke, G. H. Simon, and M. Heyde, *Phys. Rev. B* **83**, 195435 (2011).
- ¹⁴J. E. Sader and S. P. Jarvis, *Appl. Phys. Lett.* **84**, 1801 (2004).
- ¹⁵M. Heyde, M. Kulawik, H.-P. Rust, and H.-J. Freund, *Rev. Sci. Instrum.* **75**, 2446 (2004).
- ¹⁶H.-P. Rust, M. Heyde, and H.-J. Freund, *Rev. Sci. Instrum.* **77**, 043710 (2006).
- ¹⁷M. Heyde, G. H. Simon, H.-P. Rust, and H.-J. Freund, *Appl. Phys. Lett.* **89**, 263107 (2006).
- ¹⁸Note that imaging at constant Δf on the RB requires electronic modification of the setup (see, e.g., Ref. 24).
- ¹⁹S. Kawai, T. Glatzel, S. Koch, A. Baratoff, and E. Meyer, *Phys. Rev. B* **83**, 035421 (2011).
- ²⁰S. Fremy, S. Kawai, R. Pawlak, T. Glatzel, A. Baratoff, and E. Meyer, *Nanotechnology* **23**, 055401 (2012).
- ²¹It is important to note, that in order to obtain the mentioned 64 pm corrugation on the AB, one would have to chose a setpoint close to the Δf -minimum. In this case, an unintended flip to the RB is quite probable.
- ²²F. Mohn, L. Gross, and G. Meyer, *Appl. Phys. Lett.* **99**, 053106 (2011).
- ²³P. Rahe, R. Bechstein, J. Schütte, F. Ostendorf, and A. Kühnle, *Phys. Rev. B* **77**, 195410 (2008).
- ²⁴M. Heyde, M. Sterrer, H.-P. Rust, and H.-J. Freund, *Appl. Phys. Lett.* **87**, 083104 (2005).